The Role of the Endothelial Surface Glycocalyx in Solute Exchange across Capillary Walls

Masako SUGIHARA-SEKI, Takeshi AKINAGA and Tomoaki ITANO

Department of Pure and Applied Physics, Faculty of Engineering Science, Kansai University, Suita, Osaka

The luminal surface of capillary walls is covered by a layer of macromolecules referred to as the glycocalyx. In order to examine the role of the glycocalyx in the microvessel permeability, we have estimated the transport property of the microvessel wall, by using a one-dimensional model for the solute exchange through a serial pathway of the glycocalyx and the interendothelial cleft. The model provided reasonable predictions for the diffusional permeability and the reflection coefficient for solutes up to the size of albumin. The results suggest that the endothelial surface glycocalyx could form the primary molecular sieve in transcapillary pathways.

1. INTRODUCTION

The wall of capillaries is composed of a single layer of endothelial cells. The luminal surface of the endothelial cells is covered by a layer of macromolecules called the glycocalyx [1]. In our recent paper [2], we have developed a mathematical model for the exchange of solutes and suspending fluid across the endothelial surface glycocalyx and evaluated its transport properties using an idea for the membrane transport. In general, the net flux of the fluid, J_v, and solute, J_s, across a porous membrane per unit area are approximately expressed as the summation of two terms proportional to an applied concentration difference of solutes, Δc, and pressure difference, Δp, across the membrane (Kedem-Katchalsky equations) [3,4]:

$$J_s = P\Delta c + (1-\sigma)c^* J_v \,, \qquad (1a,b)$$
$$J_v = L_p(\Delta p - \sigma RT\Delta c) \,,$$

where R is the gas constant, T is the absoloute temperature and c^* is the average concentration of solutes within the passages through the membrane. The first term on the right-hand side of equation (1a) represents the diffusive transport of solutes and the second term mainly represents the convective transport. The first and second terms on the right-hand side of equation (1b) correspond to the solvent flux due to the pressure difference and the osmotic pressure, respectively. In these equations, the transport property is characterized by three parameters: P, σ and L_p. P is termed the diffusional permeability, σ is the reflection coefficient and L_p is the hydraulic conductivity.

Applying equation (1) to the solute transport through the endothelial surface glycocalyx, we have evaluated the values of the diffusional permeability and the reflection coefficient as functions of the geometry of the glycocalyx and the solute size [2]. The diffusional permeability was estimated as the value normalized by the corresponding unrestricted permeability in an unbounded region, P_0. The predicted tendencies of the relative permeability P/P_0 and the reflection coefficient σ with solute size showed satisfactory agreements with experimental results,

suggesting that the endothelial surface glycocalyx could play a major role as the size selective structure to solutes in microvessel permeability. However, experimental measurements are performed for the whole vessel wall, not just for the endothelial surface glycocalyx. In addition, the measured values of the diffusional permeability are typically normalized by the diffusion constant in an unbounded region D_0, not by P_0, since the values of P_0 are usually unknown for the whole vessel wall. Therefore, our previous comparison of the diffusional permeability with experimental measurements has been restricted to be qualitative. Thus, estimates of the diffusional permeability and the reflection coefficient for the whole pathway across the microvessel wall are necessary to make a quantitative comparison with experimental results and to confirm the conclusion of our previous study [2].

In microvessels with continuous endothelium, the principal pathway for water and small solutes lies between adjacent endothelial cells through the intercellular cleft [4]. In the present paper, therefore, we extend our study to estimate the transport property for the whole pathway across the microvessel wall, including the interendothelial cleft as well as the endothelial surface glycocalyx. As well known, the geometry of the intercellular cleft between adjacent endothelial cells is complex, so that we need detailed three-dimensional analyses for its accurate estimate. However, we here adopt the simplest one-dimensional model for the solute transport as our first approach to estimate quantitatively the diffusional permeability and the reflection coefficient. Using the estimated values for the whole microvessel wall, we shall make a comparison with experimental data of microvessels in mammalian skeletal muscle and frog mesentery, and examine the role of the endothelial surface glycocalyx in microvessel permeability to solutes.

2. MODEL AND FORMULATION

2.1 Results of the previous study [2]

Figure 1 shows a schematic view of ultrastructures of the endothelial surface glycocalyx and the intercellular cleft between adjacent endothelial cells, recently reported [5-7]. We consider the transport of solutes and fluid across the microvessel wall, through a pathway consisting of the endothelial surface glycocalyx and the intercellular cleft from the vessel lumen to the tissue space.

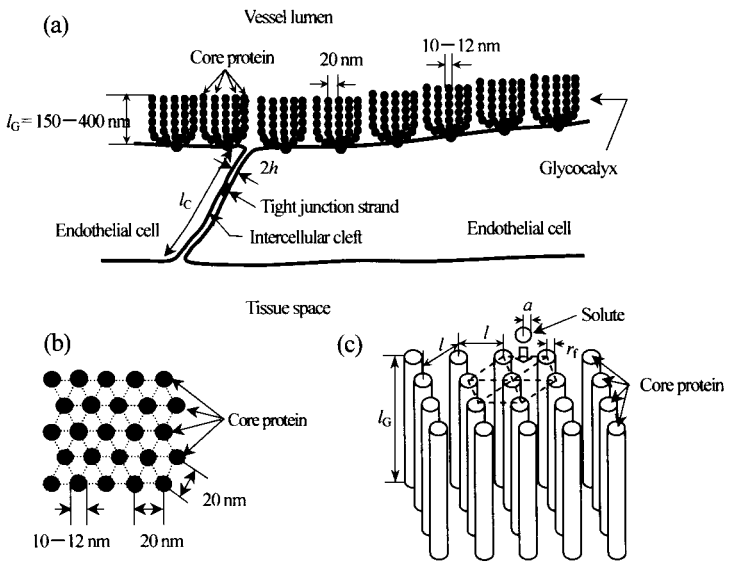

Fig. 1 (a) Sketch of the endothelial surface glycocalyx and the intercellular cleft between adjacent endothelial cells. (b) Cross-sectional view of idealized model for core proteins. (c) Model for the solute transport across the glycocalyx [2]. The core proteins are assumed to be circular cylinders with radius r_f= 6 nm, arranged parallel to each other in a hexagonal array with l = 20 nm.

From the observation by the autocorrelation imaging techniques, Squire et al.[5] proposed a structural model such that the endothelial surface glycocalyx is composed of bush-like clusters of core proteins with 10 – 12 nm diameter projecting normally to the surface of the luminal wall, and the core proteins form a two-dimensional lattice on the endothelial cell surface with 20 nm spacing (figures 1(a), (b)). As shown in figure 1(c), Sugihara-Seki[2] simplified this model by assuming core proteins as circular cylinders with radius r_f= 6 nm which align regularly parallel to each other in a hexagonal array with spacing l = 20 nm. By adopting rigid spherical particles with radius a as a solute model, steady isothermal transport of the solutes between the hexagonally arranged cylinders along their axes was formulated and analyzed when the pressure difference and the concentration difference of solutes are present across both ends of the cylinders (figure 1(c)). The length of the cylinders was assumed to be l_G = 150 – 400 nm, from experimental observations [6]. Here, we briefly summarize the results of Sugihara-Seki [2].

For the configuration shown in figure 1(c), mechanical and thermal considerations lead to approximate expressions of the relative permeability and the reflection coefficient for the glycocalyx:

$$\frac{P_G}{P_0} \approx \frac{1}{A}\int_{A^*}\frac{1}{F_t}dA\,, \quad 1-\sigma_G \approx \frac{1}{A'}\int_{A^*}\frac{F_0}{F_t}dA, \tag{2a,b}$$

where the subscript G represents the value for the glycocalyx. A is a unit area of the hexagonal cross-section perpendicular to the cylinder axis, A' is the area available for the fluid, and A^* is the area available for the center of the solute. F_t represents the drag coefficient defined as $F_t = F / 6\pi\mu aU$, where F is the drag force exerted on a solute moving with velocity U, parallel to the axis of the cylinders in an otherwise quiescent fluid, and μ is the viscosity of the fluid. Similarly, F_0 is the drag coefficient acting on a stationary solute placed in a fluid flow driven by a pressure gradient along the cylinder axis. Note that F_t and F_0 approach unity as the solute radius a tends to 0. The diffusive transport due to the pressure gradient was found to be small [2], so that the corresponding term is neglected in equation (2b).

From equation (1a), we obtain the relationship between the diffusion constant and the diffusional permeability for the glycocalyx:

$$P_G \Delta c = D_G \nabla c \quad \text{or} \quad P_G = D_G / l_G\,. \tag{3}$$

Then, in terms of the diffusion constant, equation (2a) can be rewritten as

$$\frac{D_G}{D_0} \approx \frac{1}{A}\int_{A^*}\frac{1}{F_t}dA\,, \tag{4}$$

where $D_0 = RT / 6\pi\mu aN$ and N is the Avogadro number.

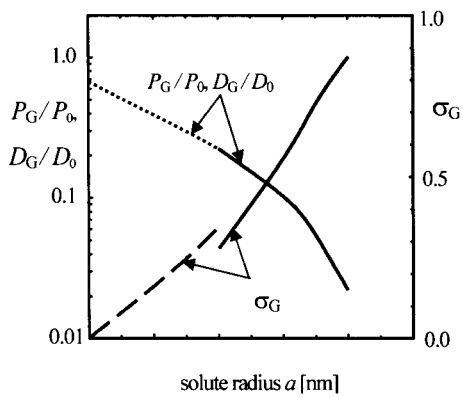

Fig. 2 The diffusional permeability normalized by the unrestricted permeability, P_G/P_0, and the reflection coefficient, σ_G, predicted by the model for the glycocalyx. The dotted curve represents P_G/P_0 obtained by the Brinkman medium approach, and the dashed curve represents $1-A^*/A'$ [2].

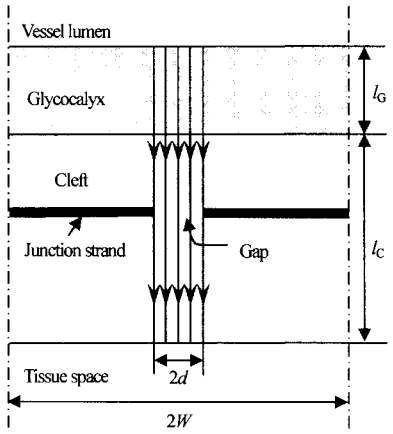

Fig. 3 Diagram illustrating the mathematical model for the solute transport across the endothelial surface glycocalyx and the interendothelial cleft. We consider one-dimensional transport limited to the gap region in the tight junction strand, as shown by straight lines with arrows.

According to equation (2), fluid mechanical computations for F_t and F_0 followed by integrations over A^* provide the values of P_G/P_0 and σ_G for the glycocalyx, as functions of the solute radius a. The results are plotted in figure 2, together with approximate estimates based on a continuum assumption or asymptotic behavior[2].

2.2 Formulation

We here consider the whole pathway of the solute transport across the microvessel wall from the vessel lumen to the tissue space. The pathway consists of the serial connection of the endothelial surface glycocalyx and the intercellular cleft between adjacent endothelial cells (see Figure 1(a)). Thus, the diffusional permeability and the reflection coefficient for the whole pathway, P_W and σ_W, can be given by [8]

$$P_W = \frac{P_G P_C}{P_G + P_C}, \tag{5}$$

$$\sigma_W = \frac{\sigma_G P_C + \sigma_C P_G}{P_G + P_C}, \tag{6}$$

where the subscript C represents the value for the intercellular cleft. Using equations (5) and (6), we shall evaluate P_W and σ_W.

As shown in figure 1(a), only small fraction of the luminal surface area of the vessel wall occupies the opening of the intercellular cleft [4]. In electron micrographs of microvessels in transverse section, the clefts are seen as narrow spaces, typically 14-21 nm wide, between the outer leaflets of adjoining endothelial cells. The width of the cleft is known to be remarkably uniform, except the region called the tight junction. The tight junctions form lines of contact between adjacent cell membranes, which are observed to run approximately parallel to the luminal and abluminal surfaces of the endothelium. They act as a barrier for the material transport, and through their discontinuities or gaps the fluid and solutes bypass the tight junctions. The morphometric analyses for rat mesentery microvessels[7] showed that the width of the cleft is approximately $2h = 18$ nm, and the cleft length per unit area of the luminal endothelial surface is $L = 0.10\ \mu m^{-1}$. The length of the gaps is reported to be $2d = 315$ nm on average and their spacing along the tight junction strand is $2W = 3590$ nm.

As an idealized mathematical model, the cleft can be treated as a two-dimensional slit between two parallel plates, in which there is a line of contact between the two plates, i.e. the tight junction strand [4,6,7,9]. Figure 3 shows the mid-plane of the cleft in the model, where the geometry is repeated periodically in the horizontal direction. We also adopt this idealized model. For simplicity, we here confine ourselves to a one-dimensional transport of solutes limited to area of the gap in the tight junction, from the vessel lumen to the tissue space, as shown by straight lines in figure 3. In other words, we consider solute transport through two-dimensional slit of

width $2h$ and length $2d$, with no spreading.

For one-dimensional transport of solutes, we obtain approximate expressions for the diffusional permeability [4]:

$$P_G^{(1)} = (2h \times 2d) \times \frac{L}{2W} \times D_G \times \frac{\phi}{l_G},$$
$$P_C^{(1)} = (2h \times 2d) \times \frac{L}{2W} \times D_C \times \frac{\phi}{l_C}, \quad (7)$$

where the superscript (1) represents the one-dimensional approximation. D_G and D_C are the solute diffusion constant within the glycocalyx and the cleft, respectively, l_G and l_C are the length of the glycocalyx and the cleft along the pathway, and ϕ is the solute partition coefficient. Here, the solute partition coefficient ϕ represents the ratio of area available for the solute center and that available for the fluid, and ϕ=1-a/h in this case. For D_G, we adopt the results of our glycocalyx model shown in figure 2, obtained from equation (4). For D_C, we use the following expression for the two-dimensional slit [4]:

$$\frac{D_C}{D_0} = 1 - 1.004\left(\frac{a}{h}\right) + 0.418\left(\frac{a}{h}\right)^3 + 0.210\left(\frac{a}{h}\right)^4 - 0.1696\left(\frac{a}{h}\right)^5. \quad (8)$$

Substituting equations (7), (8) and (4) into (5) provides the values of P_W / D_0 as a function of solute radius a.

With regard to the reflection coefficient for the cleft, σ_C, we use the following expression for the two-dimensional slit [4]:

$$\sigma_C = (1 - \phi)^2. \quad (9)$$

For σ_G, we adopt the results of our glycocalyx model shown in figure 2, obtained from equation (2b). Substituting equations (2b), (7) and (9) into (6) leads to the values of σ_W as a function of solute radius a.

3. RESULTS AND DISCUSSION

The experimental data for the diffusional permeability to hydrophilic solutes in the microcirculation of mammalian skeletal muscle [10] are shown by solid circles in figure 4. The ratios P_W/D_0 appear to decline as the solute molecular size a increases until it reaches 3.6 nm, which is the Stokes-Einstein radius of serum albumin. This tendency indicates that, although each value of P_W and D_0 decreases with solute radius, P_W falls more significantly as their molecular size increases. The decline of the ratio P_W/D_0 with molecular size was termed "restricted diffusion" [11].

Using the one-dimensional model for the solute transport, we have calculated P_W/D_0 from equations (5) and (7). The results are plotted by a solid curve in figure 4, with $2h$ = 18 nm, $2d$ = 315 nm, $2W$ = 3590 nm, L = 0.10 μm^{-1}, l_C = 411 nm, and l_G = 400 nm [7]. The results of P_W/D_0 using an approximate estimate of D_G based on the continuum assumption [2] are also plotted by a dotted curve. We notice that the P_W/D_0 curves obtained are close to the experimental data.

Our recent estimate of the hydraulic conductivity L_p using a three-dimensional model of the microvessel wall showed that the L_p values for the endothelial surface glycocalyx obtained from the three-dimensional model are significantly larger than the corresponding values obtained from the one-dimensional model. Similarly, the L_p values for the intercellular cleft from the three-dimensional model are almost twice as large as the corresponding values from the one-dimensional model. If this trend is also true for the diffusional permeability, the accord of P_W/D_0 shown in figure 4 suggests that the values of D_G and/or D_C could be smaller than the present estimate.

Experimental data of the reflection coefficient for frog mesentery capillaries [3] are shown by solid circles in figure 5. It has been found experimentally that the microvessels in many different tissues, including mesenteric capillaries and muscle microvessels, have similar values for the reflection coefficient to macromolecules [4]. In particular, Michel & Curry [4] summarized the reflection coefficient to serum albumin for various microvessels, and indicated that the measured values of σ_W are typically larger than 0.8.

The σ_W values obtained from the one-dimensional model are plotted in figure 5, with the parameter values noted in the above. Although the predicted values of σ_W in our analysis seem somewhat lower than the

experimental values for serum albumin, the present results provide better prediction than previous analyses. For example, the conventional fiber matrix theory gives $\sigma = 0.52$ or 0.67 to serum albumin, depending on the fiber radius and the spacing between the fibers[6]. Due to $P_C > P_G$ obtained in the current model, equation (6) indicates a larger contribution of the endothelial surface glycocalyx to σ_W than the intercellular cleft. However, a much more contribution of the glycocalyx to the reflection coefficient may be expected, since a comparison between figures 2 and 5 shows that the values of σ_G for the endothelial surface glycocalyx alone can explain the experimental measurements better than those of σ_W for the whole vessel wall in the current one-dimensional model.

The difference between our results and experimental measurements may be partly explained by the presence of the electrical negative charge on the surfaces of serum albumin, which interacts with the negative charge on the glycocalyx. The repulsive interaction between the electrical charges can be shown to increase the reflection coefficient, depending on the amount of electrical charges, the size of solutes and the icon concentration of the fluid [12]. Furthermore, the fact that albumin is an ellipsoidal and not a spherical molecule may affect the reflection coefficient. Inclusion of these effects is necessary for more comprehensive understanding about the transport property of the microvessel wall.

4. CONCLUSIONS

The solute transport across microvessel walls is studied using a mathematical model developed for the endothelial surface glycocalyx as well as the intercellular cleft. Although the current model is an idealized one-dimensional one, it could account plausibly for the experimentally measured values of the diffusional permeability and the reflection coefficient to macromolecules. The results suggest that the endothelial surface glycocalyx could play a major role in solute transport. More detailed three-dimensional model taking into account the ultrastructure of the microvessel wall is necessary to elucidate the transport property of the microvessel wall.

Acknowledgement This research has been supported in part by Grand-in-Aid for Scientific Research (B) 16360093 and 16360090.

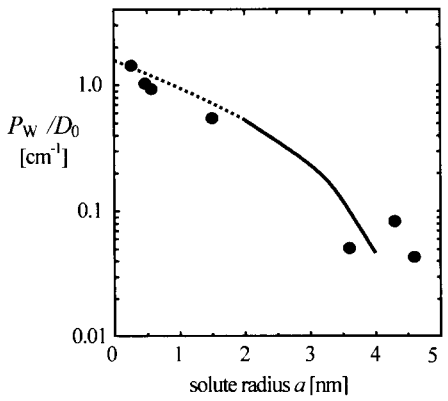

Fig. 4 The restricted diffusion P_W / D_0 for microvessels in mammalian skeletal muscle [10] (solid circles). The solid and dotted curves represent P_W / D_0 estimated from equations (5), (7) and (8) together with the results for the glycocalyx shown in figure 2.

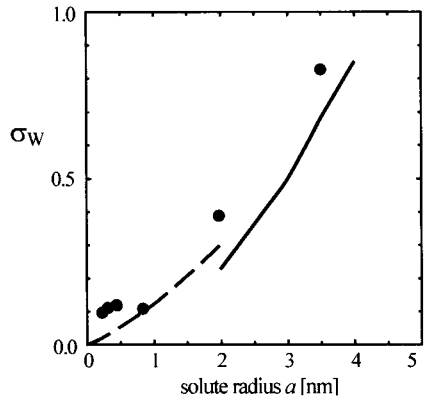

Fig. 5 The reflection coefficient σ_W obtained by experimental measurements for frog mesentery capillaries [3] (solid circles). The solid and dashed curves represent σ_W estimated from equations (6), (7) and (9) together with the results for the glycocalyx shown in figure 2.

REFERENCES

1) Pries, A.R., Secomb, T.W. and Gaehtgens, P., "The endothelial surface layer", *Pflügers Archiv: Eur. J. Physiol.* **440** (2000), pp.653-666.
2) Sugihara-Seki, M., "Transport of spheres suspended in the fluid flowing between hexagonally arranged cylinders", *J. Fluid Mech.* **551** (2006), pp.309-321.
3) Curry, F.E., "Mechanics and thermodynamics of transcapillary exchange", In: *Handbook of Physiology* (Am. Physiol. Soc., 1984), vol. 4 part 1, pp.309-374.
4) Michel, C.C. and Curry, F.E., "Microvascular permeability", *Physiol. Rev.* 70 (1999), pp.703-761.
5) Squire, J.M., Chew, M., Nneji, G., Neal, C., Barry, J. and Michel, C., "Quasi-periodic substructure in the microvessel endothelial glycocalyx: a possible explanation for molecular filtering?" *J. Struc. Biol.* 136 (2001), pp.236-255.
6) Weinbaum, S., Zhang, X., Han, Y., Vink, H. and Cowin, S., "Mechanotransduction and flow across the endothelial glycocalyx", *PNAS* 100 (2003), pp.7988-7995.
7) Adamson, R.H., Lenz, J.F., Zhang, X., Adamson, G.N., Weinbaum, S. and Curry, F.E., "Oncotic pressures opposing filtration across non-fenestrated rat microvessels", *J. Physiol.* 557 (2004), pp.889-907.
8) Fu, B.M., Weinbaum, S., Tsay, R.Y. and Curry, F.E., "A junction-orifice-fiber entrance layer model for capillary permeability: application to from mesenteric capillaries", *Transactions of the ASME J. Biomech., Eng.* 116 (1994) pp.502-513.
9) Renkin, E.M., "Transport pathways and processes", In: *Endothelial Cell Biology in Health and Disease*, (edited by N. Simionescu & M. Simionescu) (Plenum Press, 1988), pp.51-68.
10) Pappenheimer, J.R., Renkin, E.M. and Borrero, J.M., "Filtration, diffusion and molecular sieving through peripheral capillary membranes. A contribution to the pore theory of capillary permeability", *Am. J. Physiol.* 167 (1951), pp.13-46.
11) Levitt, D.G., "General continuum analysis of transport through pores. II. Nonuniform pores", *Biophys. J.* 15 (1975), pp.553-563.
12) Akinaga, T., Sugihara-Seki, M., and Itano, T., "An electrostatic model for osmotic flow through charged pores", In: *5th World Congress of Biomechanics*, (edited by D. Liepsch Ed.) (Medimond S.r.l., 2006) ISBN 88-7587-271-6, G729C2335.